ELSEVIER

Journal of Alloys and Compounds 396 (2005) 79–85

Journal of ALLOYS AND COMPOUNDS

www.elsevier.com/locate/jallcom

Optical transition properties of Yb^{3+} in new fluorophosphate glasses with high gain coefficient

Ju H. Choi[a], Alfred Margaryan[b], Ashot Margaryan[b], Frank G. Shi[a,*]

[a] *Optoelectronic Integration and Packaging Laboratory, Department of Chemical Engineering and Material Science, University of California, Irvine, CA 92697, USA*

[b] *AFO Research Inc., Glendale, P.O. Box 1934, CA 91209, USA*

Received 9 August 2004; received in revised form 25 October 2004; accepted 28 October 2004
Available online 25 January 2005

Abstract

A new series of $0.4MgF_2$–$0.4BaF_2$–$0.1Al(PO_3)_3$–$0.1Ba(PO_3)_2$ glasses doped with Yb^{3+} is introduced for fiber and waveguide laser applications. Spectroscopic properties including emission cross-section and lifetime and optical properties including refractive index, nonlinear refractive index, and Abbe number are reported as a function of Yb_2O_3 concentration. The refractive index n_d is linearly dependent on Yb_2O_3 concentration, while the nonlinear refractive index, $n_2 = 1.42 \times 10^{-13}$ esu, which is independent of Yb_2O_3 concentration, is extremely small. In addition, the Abbe number is remarkably high, >65, and is also independent of Yb_2O_3 concentration. To our knowledge, the emission cross-section σ_{emi}, which was found to be ~0.87 pm^2 at the lasing wavelength of 996 nm, is the highest one among fluorophosphate glasses. This glass exhibits an extremely high gain coefficient, $G = 0.95$ ms pm^4, and high quantum efficiency of $\eta = 94\%$. The combination of outstanding spectroscopic (high emission cross-section and gain coefficient) and optical (low dispersion and small nonlinear refractive index) properties demonstrates that the current Yb^{3+} activated fluorophosphate glass is an excellent candidate material for fiber and waveguide lasers.

Keywords: Fluorophosphate glass; Spectroscopic property

1. Introduction

Recent innovations in special photonic glasses and fibers are pushing fiber lasers to the forefront of solid-state laser applications and consequently an on-going reshaping of the laser industry [1]. Glasses doped with rare earth ions are the material foundation for fiber lasers and amplifiers. Among rare earth ions, Yb^{3+} ion is important for diode pumped solid-state lasers because of its simple $^2F_{5/2}$–$^2F_{7/2}$ transition [2]. Yb^{3+} doped laser glasses are attractive for high power lasers to be needed for next-generation nuclear fusion and as a sensitizer of energy transfer for infrared to visible up-conversion and infrared laser [3].

Among potential active dopant host materials, fluorophosphate glasses are promising because of its potential for hosting various rare earth dopants [4–9]. Fluorophosphates glasses can also offer improved optical properties, such as low nonlinear refractive index, low phonon energy, and high transparency from near UV to mid-IR [10–12]. For fiber lasers, it is desirable for the emission cross-section (σ_{emi}) to be as large as possible in order to achieve a high gain for a short length of fiber and for compact planar waveguide lasers or microchip lasers. The fluorescence lifetime (τ_f) is also desired to be as long as possible in order to permit a greater pulsed power. Unfortunately, the reported fluorophosphate glasses have a low emission cross-section, i.e., <0.5 pm^2, which is not sufficient for the diode-pumped short pulse laser applications [13–15]. In order to improve emission cross-section, the addition of various network formers and the variation of chemical compositions have been performed, which could change the asymmetry of Yb^{3+} and the covalence between Yb^{3+} and ligand [16].

The purpose of this work is to introduce the novel alkali-free fluorophosphate glass with a high gain for fiber and waveguide laser applications. A systematic investigation of

* Corresponding author. Tel.: +1 949 824 5362; fax: +1 949 824 2541.
E-mail address: fgshi@uci.edu (F.G. Shi).

0925-8388/$ – see front matter © 2004 Elsevier B.V. All rights reserved.
doi:10.1016/j.jallcom.2004.10.076

dependence of Yb^{3+} concentration on the optical and spectroscopic properties is performed. The optical properties including refractive index (n), dispersion, i.e., Abbe number (ν_d) are determined. The absorption and emission spectra for Yb^{3+}-doped fluorophosphate glasses are measured in order to assess their capabilities of being used as fiber and waveguide lasers. Gain coefficient (G), the quantum efficiency (η) and the minimum pumping intensity (I_{min}) are determined to find the optimized concentration and to evaluate the laser performance.

2. Experiment procedure

2.1. Glass synthesis

Starting materials are from MgF_2, BaF_2, $Al(PO_3)_3$ and $Ba(PO_3)_2$ (City Chemicals) and Yb_2O_3 (Spectrum Materials) with a purity of above 99.99%. A series of starting materials were weighed according to $0.4MgF_2$–$0.4BaF_2$–$0.1Al(PO_3)_3$–$0.1Ba(PO_3)_2$ glasses on 0.1% accuracy and mixed thoroughly. The mixed raw materials were melted in a vitreous carbon crucible in Ar-atmosphere at 1200–1250 °C for 1 h. The quenched samples were annealed at 410 °C for 20 h to remove internal stress. The residual stress was examined by the polariscope (Rudolph Instruments). Samples were cut and polished by the size of 15 mm × 10 mm × 2 mm for optical and spectroscopic measurements.

2.2. Spectroscopic property measurement

The refractive index (n_D, n_F and n_C) was measured with a unit of Abbe refractometer (ATAGO) at 20 °C at the wavelength of 486.1, 589, and 656.3 nm, respectively. The absorption spectra were measured by Perkin-Elmer (Lambda 900) spectrometer in the range of 800–1200 nm at room temperature. The emission spectra, stimulated by 950 nm Ti–sapphire laser excited by Ar-laser, were focused onto a monochromator with a 1200 line/mm grating at room temperature. The fluorescence spectra are then recorded over the range 800–1200 nm using a monochromator (Oriel) and a Si pin detector (Thorlabs). The laser radiation incident to the sample was passed through an optical chopper (Stanford Research) enabling the use of a lock-in amplifier (Ametek 5105) to recover and amplify the electronic signal from the detector. The lifetime of the excited state was determined with a Q-switched Nd–YAG laser pumping an OPO (Continuum Surelite). The duration of the pulses was 5 ns. The fluorescent radiation is detected using a Si pin photodiode (Thorlabs) via an interference filter (Edmund Scientific). The signal was amplified with a recorded with a fast oscilloscope (LeCroy 9350) and transferred to a computer, where it is fitted to an exponential.

3. Data analysis

3.1. Optical properties

Optical dispersion of optical glasses is normally represented by the Abbe number (ν_d) by the following relationship:

$$\nu_d = \frac{n_D - 1}{n_F - n_C} \tag{1}$$

where n_D, n_F, and n_C are the refractive indices at the D, C and F spectral lines. Refractive index (n) consists of linear refractive index (n_d) and non-linear refractive index (n_2) in electromagnetic intensity (I), i.e., $n = n_d + n_2 I$. The nonlinear refractive index (n_2) units can be determined by the following relationship [17]:

$$n_2[\text{esu}] = \frac{K(n_d - 1)(n_d^2 - 2)^2}{\nu_d\sqrt{1.517 + (n_d^2 + 2)(n_d + 1)\nu_d/6n_d}} \tag{2}$$

where c and n_o are the speed of light and linear refractive index, respectively. The value of K is an empirical factor that might be constant; 70×10^{-13} esu for fluoride glasses [17]. In this work, K of 70×10^{-13} esu was used to estimate n_2, because major compositions are mostly composed of (Mg, Ba)F_2.

3.2. Spectroscopic properties

From the absorption spectra, the spontaneous transition probability (A_{ra}) is experimentally determined by using following relationship [18]:

$$A_{ra} = \frac{8\pi cn(\lambda_p)^2(2J' + 1)}{\lambda_p^4(2J + 1)} \int k(\lambda)\,d\lambda \tag{3}$$

where J' and J are the total momentum for the upper and lower levels, respectively, λ_p the absorption peak wavelength, $k(\lambda)$ the absorption coefficient at the absorption wavelength λ, and $n(\lambda_p)$ is the refractive index at each absorption peak wavelength which was determined by using Cauchy's equation, $n(\lambda) = A + B/\lambda^2$. The absorption cross-section can be obtained by using Eq. (4) [19], i.e.,

$$\sigma_{abs} = \frac{2.303\,\log(I_0/I)}{NL} \tag{4}$$

where N is the Yb^{3+} ion concentration (ion/cm^3) and L is the thickness of the sample. There are two most usual methods to determine the emission cross-section (σ_{emi}) for the $^2F_{5/2}$–$^2F_{7/2}$ transition of Yb^{3+}. The one to obtain the emission cross-section (σ_{emi}) using integrated absorption cross-section ($\int k(\lambda)\,d\lambda$) was given by the Fuchtbauer–Landenburg Eq. (5) [19], i.e.,

$$\sigma_{em} = \frac{\lambda_p^4 A_{ra}}{8\pi cn(\lambda_p)^2 \Delta\lambda_{eff}} = \frac{4\int k(\lambda)\,d\lambda}{3\Delta\lambda_{eff}} \tag{5}$$

where λ_p is the wavelength of the absorption peak, c the speed of light in vacuum, $n(\lambda_p)$ the refractive index at emission peak wavelength, and $\Delta\lambda_{eff}$ is effective fluorescence linewidth. The latter is the reciprocity method based on McCumber (6) [18,20],

$$\sigma_{emi}(\lambda) = \sigma_{abs}(\lambda)\frac{Z_l}{Z_u}\exp\left(\frac{E_{Zl} - hc\lambda^{-1}}{kT}\right) \quad (6)$$

where Z_l, Z_u, and k are the partition functions of the lower, upper levels, and the Boltzmann's constant, respectively. The reciprocity method may be employed for host materials with appropriate energy level data. The zero line energy E_{Zl}, which is defined to be the energy separation between the lowest components of the upper and lower field states, is associated with the strongest peak in absorption spectra of Yb^{3+}. In the high temperature limit, the ratio of Z_l/Z_u becomes the degeneracy weighting of the two states corresponding to the $^2F_{7/2}$–$^2F_{5/2}$ transition [18]. Since the ratio of Z_l/Z_u does not change distinctively with respect to various glass materials, thus the value of Z_l/Z_u has been 4/3 at room temperature [21].

3.3. Laser parameters

In order to assess the potential of the real Yb^{3+} doped glass as a laser material, several important parameters such as the minimum pumping intensity (I_{min}), the minimum fraction of excited ions (β_{min}) and the saturation pumping intensity (I_{sat}) should be determined. The minimum absorbed pumping intensity (I_{min}), which is required for the transparency to be achieved at the lasing wavelength (λ_0), is calculated by the following Eqs. (7) and (8) [22],

$$I_{min} = \beta_{min} \times I_{sat} \quad (7)$$

and β_{min} is given by

$$\beta_{min} = \frac{\sigma_{abs}(\lambda_0)}{\sigma_{emi}(\lambda_0) + \sigma_{abs}(\lambda_0)} = \left\{1 + \frac{Z_l}{Z_u}\exp\left[\frac{(E_{Zl} - hc\lambda_0^{-1})}{kT}\right]\right\}^{-1} \quad (8)$$

In Eq. (8), $\sigma_{abs}(\lambda_0)$ and $\sigma_{emi}(\lambda_0)$ represent the absorption and the emission cross-section at the lasing wavelength (λ_0),

$$I_{sat} = \frac{hc}{\lambda_p \tau_f \sigma_{abs}(\lambda_p)} \quad (9)$$

where λ_p and τ_f represent the excitation wavelength and the fluorescence lifetimes after fitting the measured values to the first order exponentials, and $\sigma_{abs}(\lambda_p)$ is the absorption cross-section at the absorption wavelength.

The gain coefficient (G, $\sigma_{abs}(\lambda_p) \times \tau_f \times \sigma_{emi}$) is closely related to the product of absorption cross-section $\sigma_{abs}(\lambda_p)$, emission cross-section (σ_{emi}) and fluorescence lifetime (τ_f) as below [23]:

$$G = N^* \times \sigma_{emi} \quad (10)$$

$$N^* = N \times E_p \times \sigma_{abs}(\lambda_p) \times t_f \quad (11)$$

$$G = N \times E_p \times \sigma_{abs}(\lambda_p) \times \tau_f \times \sigma_{emi} \propto \sigma_{abs}(\lambda_p) \times \sigma_{emi}\tau_f \quad (12)$$

where N^*, N, E_p are the inversion population number, rare earth dopant concentration, and pump energy independent of host, respectively. Therefore, the gain coefficient (G) is proportional to $\sigma_{abs}(\lambda_p) \times \sigma_{emi} \times \tau_f$. The product of absorption cross-section $\sigma_{abs}(\lambda_p)$ and fluorescence lifetime (τ_f) is proportional to the stored energy and one of the emission cross-section (σ_{emi}) and fluorescence lifetime (τ_f) is proportional to extraction efficiency. The higher stored energy and extraction efficiency gives better potentials for laser host materials. It, therefore, has been suggested that the laser glass should have high gain coefficient (G) for laser applications.

4. Results

4.1. Optical properties

Fig. 1 shows the wavelength dependence of refractive index for Yb^{3+}-doped $0.4MgF_2$–$0.4BaF_2$–$0.1Al(PO_3)_3$–$0.1Ba(PO_3)_2$ fluorophosphate glasses. It is observed that the refractive index increases as Yb_2O_3 with high atomic weight increases, but the refractive index decreases as the wavelength of spectral line increases from 486 to 589 and 656 nm.

The dopant concentration dependence for both nonlinear refractive index (n_2) and Abbe number (ν_d) are presented in Fig. 2. Abbe number (ν_d) can be used to classify optical glasses and to indicate the degree of light dispersion. Abbe number (ν_d) for the undoped fluorophosphate glass is 68.27. For Yb^{3+}-doped fluorophosphate glasses, Abbe numbers slightly decrease to 65.31, but it remains constant around 65.31–67.5. Nonlinear refractive index (n_2) for the undoped fluorophosphate glass, which is theoretically calculated using Eq. (7), is found to be 1.3308×10^{-13} esu and then slightly increases to 1.4244×10^{-13} esu at 1 wt% Yb_2O_3.

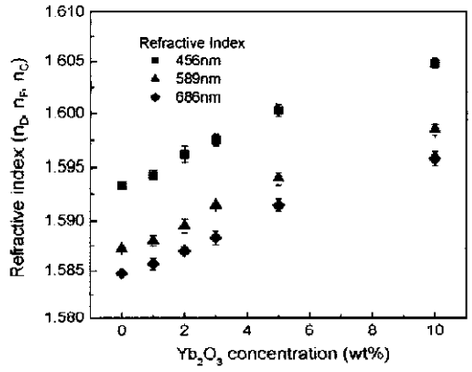

Fig. 1. Dependence of refractive index on Yb_2O_3 concentration.

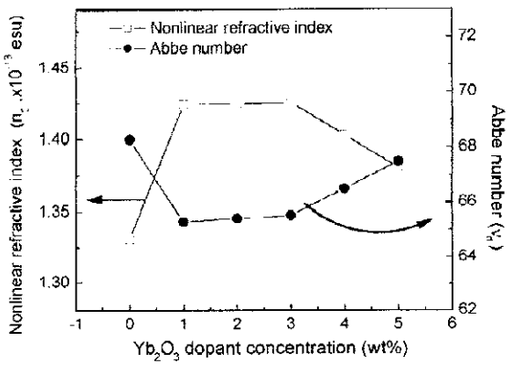

Fig. 2. Dependence of Abbe number (ν_d) and nonlinear refractive index (n_2) on Yb_2O_3 concentration. Lines are drawn as a guide for eyes.

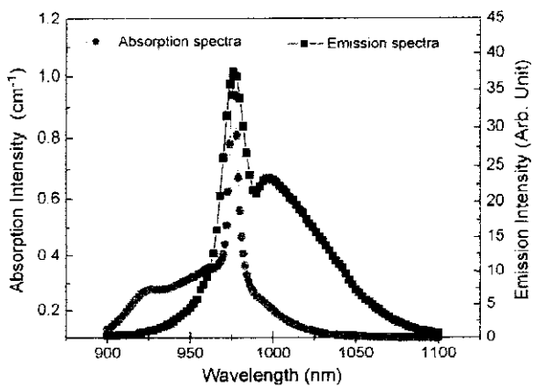

Fig. 3. Absorption and emission spectra of Yb^{3+} in the new fluorophosphates glass doped with 4 wt% Yb_2O_3.

The overall nonlinear refractive index (n_2) still remains between 1.3308×10^{-13} and 1.4254×10^{-13} esu which is one order smaller than oxide glasses [24].

4.2. Spectroscopic properties

Fig. 3 shows the emission and absorption spectra of Yb^{3+} in fluorophosphate glass doped with 3 wt% Yb_2O_3. The center peak of absorption of the $^2F_{7/2} \rightarrow {}^2F_{5/2}$ transition is located at 976 nm and the peaks of emission bands are located at 977 and 996 nm. Table 1 lists some of the spectroscopic properties of Yb^{3+}-doped fluorophosphate glasses at room temperature as a function of Yb_2O_3 concentration. As shown in Table 1, there is a systematic variation with Yb_2O_3 concentration. The absorption cross-section ($\sigma_{abs}(\lambda_p)$), the emission cross-section ($\sigma_{cmi}(\lambda_0)$) and the spontaneous transition probability (A_{rad}) and fluorescence effective linewidth ($\Delta\lambda_{eff}$) increase with an increase in Yb_2O_3 concentration. Radiative lifetime (τ_{rad}) calculated from the spontaneous transition probability (A_{rad}) and quantum efficiency (η) shows the linear increase.

4.3. Laser properties

Fig. 6 shows the relationship product of absorption cross-section and fluorescence lifetime ($\sigma_{abs}(\lambda_p) \times \tau_f$) and saturation pumping intensity (I_{sat}). The various concentration effects on laser performance properties including minimum pumping intensity (I_{min}), the minimum fraction of excited ions (β_{min}) and the saturation pumping intensity (I_{sat}) are explained as Yb_2O_3 concentration increases. The product of absorption cross-section and fluorescence lifetime ($\sigma_{abs}(\lambda_p) \times \tau_f$) almost linearly decreases from 1.43 to 0.69 ms pm^2 and saturation pumping intensity (I_{sat}) increases from 18.12 to 37.7 kW/cm^2 with increasing Yb_2O_3 concentration.

Fig. 7 shows the variation of the minimum pump intensity (I_{min}) and gain coefficient (G) as a function of Yb_2O_3 concentration. Gain coefficient (G), i.e., the stored energy and extraction efficiency, linearly falls from 9.6 to 0.25 ms pm^4 and minimum pump intensity (I_{min}), which shows the ease of pumping the material to achieve laser action, dramatically rise from 3.1 to 8.15 kW/cm^2 with increasing Yb_2O_3.

5. Discussion

5.1. Linear and nonlinear refractive index

The wavelength dependence of refractive index for Yb^{3+}-doped $0.4MgF_2$–$0.4BaF_2$–$0.1Al(PO_3)_3$–$0.1Ba(PO_3)_2$ fluorophosphate glasses are shown in Fig. 1. The refractive index of a glass is mainly dependent on individual polarizabilities of cation ions and the concentration of cation per unit volume. The refractive index, generally, also increases with increasing size of cation [25]. Considering that the host materials in this work are fixed and mainly composed of $0.4MgF_2$–$0.4BaF_2$–$0.1Al(PO_3)_3$–$0.1Ba(PO_3)_2$

Table 1
Spectroscopic properties of Yb^{3+}-doped fluorophosphate glasses at room temperature as a function of Yb_2O_3 concentration

Yb_2O_3 (wt%)	n_d	λ_{ZI} (nm)	$\sigma_{abs}(\lambda_p)$ (pm^2)	A_{rad} (sec^{-1})	$\sigma_{emi}(\lambda_0)$ (pm^2)	$\Delta\lambda_{eff}$ (nm)	τ_{rad} (ms)	η (%)
1	1.5476	976	1.643	1456	0.87	84.42	0.65	94
2	1.5486	976	1.606	1259	0.74	85.69	0.79	73
3	1.5490	976	1.511	1239	0.69	85.80	0.84	55
4	1.5519	976	1.457	991	0.51	87.38	1.12	36
5	1.5549	976	1.470	833	0.47	88.88	1.2	29

fluorophosphate, the refractive index is to be mainly determined by the concentration of Yb^{3+} per unit volume. The increase of refractive index in these glass systems is mainly attributed to Yb_2O_3 with high ionic polarizability. A work related to the dependence of linear refractive index on the several rare earth dopants and their concentration will be discussed in detail in previous work using molar volume (V_m) and molar refractivity (R_m) [26].

Generally, there is an inverse relationship between the Abbe number and refractive index in optical glasses. In other words, the glass with high refractive index is supposed to have relatively low Abbe number, i.e., a high dispersion. It is remarkable that, Fig. 2 shows that the refractive index increases linearly with the concentration of Yb_2O_3 but ν_d do not noticeably decline with increasing Yb_2O_3 concentration. In comparing with other fluorophosphate glasses with ν_d being in the range of 45–75 [27], they remain to be almost constant in the range of 65.31–67.5. It indicates that the dispersion is still low and not significantly affected by Yb_2O_3 concentration. It is due to the fact that the dependence of partial dispersion ($n_F - n_C$) and n_D on wavelength is almost that same, i.e., the varying ratio of refractive index according to wavelength is not significantly different with Yb_2O_3 concentration.

The knowledge of low nonlinear refractive index (n_2) is required for laser applications to prevent spatial intensity fluctuations in the wavefront and self-focusing which lead to damage of optical components [28]. Nonlinear refractive index (n_2) can be also mainly affected by the refractive index or polarizability of the glass constituents. Nonlinear refractive index (n_2) is inversely dependent on ν_d, and exponentially increases with n_d as shown in Eq. (2). It increases up to 1.424×10^{-13} esu at 1 wt% Yb_2O_3, and then slightly decreases as Yb_2O_3 concentration increases. While the increase of refractive index (n_d) linearly increases due to an increase of Yb_2O_3 concentration, it is interesting that nonlinear refractive index (n_2) remains constant as ν_d decreases. Consequently, the nonlinear refractive index (n_2) is found to be not strongly affected by its concentration.

5.2. Relationship between the integrated absorption cross-section ($\int \sigma_{abs}\, d\lambda$) and emission cross-section (σ_{emi})

The relationship between the integrated absorption cross-section ($\int \sigma_{abs}\, d\lambda$) and emission cross-section (σ_{emi}) for Yb^{3+} doped fluorophosphates glasses is shown in Fig. 4. As shown in Eq. (5) above, the emission cross-section (σ_{emi}) is closely related to the integrated absorption cross-section ($\int \sigma_{abs}\, d\lambda$). Linearity between them is observed in Fig. 4, which indicates that the emission cross-section (σ_{emi}) strongly depends on integrated absorption cross-section ($\int \sigma_{abs}\, d\lambda$). Emission cross-section (σ_{emi}) obtained through Fuchtbauer–Ladenburg method is to be assessed again for the reasonableness by using reciprocity method i.e., Eq. (6). The discrepancies between two values of emission

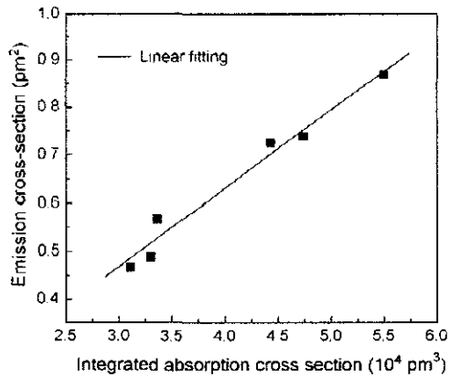

Fig. 4. Relationship between the integrated absorption cross-section ($\sigma_{abs}(\lambda_p)$) and the emission cross-section.

cross-section are found to be below 15%, which shows that both methods are effective and appropriate for the determination of emission cross-section (σ_{emi}).

5.3. Dependence of spectroscopic properties on Yb^{3+} concentration

The absorption spectra are normalized from the optical density by the sample thickness and also Yb^{3+} concentration. As shown in Table 1, the absorption cross-section ($\sigma_{abs}(\lambda_p)$) at zero line absorption peak and spontaneous transition probability (A_{rad}) of the $^2F_{7/2} \rightarrow {}^2F_{5/2}$ transition exhibit a maximum at 1 wt% Yb_2O_3 and then monotonically decrease with an increase in Yb_2O_3 concentration. The fluorescence lifetime (τ_f) of Yb^{3+} from upper laser level linearly shortens from 0.67 to 0.36 ms with an increase from 1 to 5 wt% Yb_2O_3 concentration, which indicates that the quenching effect of lifetime (τ_f) of Yb^{3+} exists. It is obvious that quenching effect of Yb^{3+} ion in this system exist. The maximal intensity of fluorescence at 4 wt% was observed and then lessened gradually. The concentration quenching above 4 wt% Yb_2O_3 might be due to energy migration between Yb^{3+} ions and energy transfer to certain impurities. The mechanism on quenching of Yb^{3+} ions in this system will be discussed in another work. Table 2 lists some of the spectroscopic properties; the absorption cross-section ($\sigma_{abs}(\lambda_0)$), fluorescence lifetime (τ_f) and the figure of merit ($\tau_f \times \sigma_{emi}$) with some reported glasses. The figure of merit present that the fluorophosphate glasses has an advantage over some fluorophosphate based glasses.

Fig. 5 shows the variation of the integrated absorption coefficient ($\int k(\lambda)\, d\lambda$) and effective linewidth ($\Delta\lambda_{eff}$) as a function of Yb_2O_3 concentration. The emission cross-section (σ_{emi}) which is determined by the Fuchtbauer–Ladenburg method at 996 nm, monotonically decreases with increasing Yb^{3+} concentration. Based on the Fuchtbauer–Ladenburg method, the emission cross-section (σ_{emi}) is determined by the integrated absorption cross-section ($\int k\, d\lambda$) and effective linewidth ($\Delta\lambda_{eff}$). According to relationship between the

Table 2
Comparisons of spectroscopic properties compared with some fluorophosphate glasses with high fluorine

Host glasses	n_d	λ_{ZI} (nm)	$\sigma_{abs}(\lambda_0)$ (pm^2)	$\sigma_{emi}(\lambda_0)$ (pm^2)	τ_f (ms)	$\tau_f \times \sigma_{emi}$ (ms pm^2)	Reference
FP[a]	≅1.5	1020	0.43 (p)	0.5	1.2	0.6	[14]
FP	≅1.5	970	0.4	0.2	1.3	0.26	[15]
FP15	1.472	1001	-	0.49	1.6	0.78	[27]
Current system Yb_2O_3 1 wt%	1.5476	976	0.29	0.87	0.65	0.57	This work

integrated absorption cross-section ($\int \sigma_{abs}\, d\lambda$) and emission cross-section (σ_{emi}) in Fig. 4, it is evident that the increase of integrated absorption coefficient ($\int k\, d\lambda$) gives rise to an increase in the emission cross-section (σ_{emi}). On the other hand, the effective linewidth ($\Delta\lambda_{eff}$) is the slight increase in the effective linewidth ($\Delta\lambda_{eff}$) leads to a decrease in the emission cross-section (σ_{emi}) as Yb^{3+} concentration increases. Consequently, the counterbalance of two effects between integrated absorption cross-section ($\int k\, d\lambda$) and the effective linewidth ($\Delta\lambda_{eff}$) leads emission cross-section (σ_{emi}) not to a noticeable decreasing with an increase in Yb_2O_3 concentration.

5.4. Laser parameters

Relationship between the product of the absorption cross-section and fluorescence lifetime ($\sigma_{abs}(\lambda_p) \times \tau_f$) and saturation pumping intensity (I_{sat}) is shown in Fig. 6 as a function of Yb_2O_3 concentration. When the product of the absorption cross-section and fluorescence lifetime ($\sigma_{abs}(\lambda_p) \times \tau_f$) becomes lower, the saturation pumping intensity (I_{sat}) linearly increases along with increasing Yb_2O_3, which is consistent with Eq. (9). In other words, it is desirable for the saturation pumping intensity (I_{sat}) to be as low as possible to minimize the minimum pumping intensity (I_{min}) since the emission cross-section ($\sigma_{emi}(\lambda_p)$) is proportional to ($\sigma_{abs}(\lambda_p)$) as shown in Eq. (6). Incidentally, the minimum fraction of excited ions (β_{min}) does not change very much with increasing Yb_2O_3 concentration. It is, thus, apparent for minimum pumping intensity (I_{min}) closely to be proportional to saturation pumping intensity (I_{sat}) following Eq. (7).

Dependence of the gain coefficient (G) and the minimum pump intensity (I_{min}) on Yb_2O_3 concentration is shown in Fig. 7. The gain coefficient (G) is entirely used to evaluate the laser performance in terms of stored energy and extraction efficiency. It is apparent that the exponential decrease of the gain coefficient (G) results from the decrease of the absorption cross-section ($\sigma_{abs}(\lambda_p)$), emission cross-section (σ_{emi})

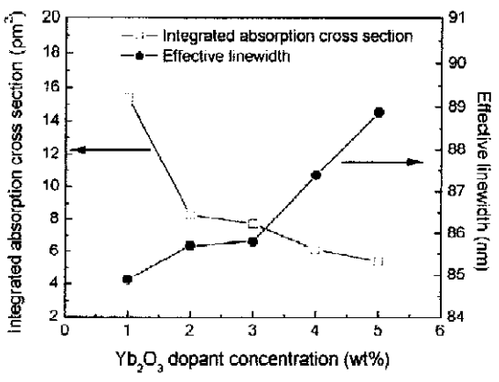

Fig. 5. Integrated absorption cross-section ($\int k\, d\lambda$) and effective linewidth ($\Delta\lambda_{eff}$) as a function of Yb_2O_3 concentration. Lines are drawn as a guide for eyes.

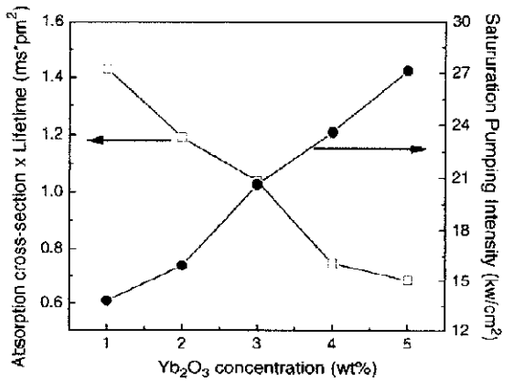

Fig. 6. Relationship between the product of the absorption cross-section and fluorescence lifetime ($\sigma_{abs}(\lambda_p) \times \tau_f$) and saturation pumping intensity (I_{sat}) as a function of Yb_2O_3 concentration. Lines are drawn as a guide for eyes.

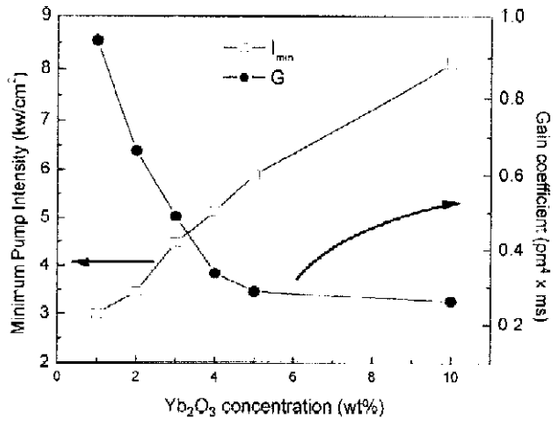

Fig. 7. Dependence of the gain coefficient (G) and the minimum pump intensity (I_{min}) on Yb_2O_3 concentration. Lines are drawn as a guide for eyes.

and the fluorescence lifetime (τ_f) with an increase of Yb_2O_3 concentration. In this glass system, the concentration quenching of Yb^{3+} is observed, but the value of gain coefficient (G) has also some advantages over some fluorophosphate glasses [29].

6. Conclusions

A new series of $0.4MgF_2$–$0.4BaF_2$–$0.1Al(PO_3)_3$–$0.1Ba(PO_3)_2$ glasses doped with Yb^{3+} has successfully been developed. A systematic investigation of optical properties including refractive index (n), Abbe number (ν_d) and nonlinear refractive index (n_2) have been performed as a function of Yb_2O_3 concentration. The best laser performance is found in the fluorophosphate glass doped with 1 wt% Yb_2O_3, i.e., 1.265×10^{20} ions/cm^3. The lifetime (τ_f) is found to be 0.67 ms. The low dispersion of $\nu_d = 65.3$ and low nonlinear refractive index of $n_2 = 1.42 \times 10^{-13}$ esu are obtained. This system exhibits a high gain coefficient of $G = 0.95$ ms pm^4 and a high quantum efficiency of $\eta = 94\%$. The favorable combination of outstanding spectroscopic and optical demonstrates that the current Yb^{3+} activated fluorophosphate glass is an excellent candidate material for fiber and waveguide lasers.

Acknowledgements

The authors would like to thank J. H. Song and Professor J. Heo in Postech, Korea for experiments.

References

[1] S. Woods, Laser Focus Worlds 39 (6) (2003) 85.
[2] D. Pearson, S.P.S. Porto, Appl. Phys. Lett. 4 (1964) 202.
[3] B. Peng, T. Izumitani, Rev. Laser Eng. 21 (1993) 1234.
[4] J.F. Philips, T. Topfer, H. Ebendorff-Heidepriem, D. Ehrt, R. Sauerbrey, Appl. Phys. B 72 (2001) 399.
[5] H. Ebendorff-Heidepriem, D. Ehrt, J. Philips, T. Topfer, A. Speghini, M. Bettinelli, R.W. Sun Fat, Proc. SPIE 3942 (2000) 29.
[6] O. Deutschbein, M. Faultisch, W. Jahn, G. Krolla, N. Neuroth, Appl. Opt. 17 (1978) 2228.
[7] J.H. Choi, F.G. Shi, A. Margaryan, A. Margaryan, W.E. van der Veer, Proc. SPIE 4974 (2003) 106.
[8] J.H. Choi, F.G. Shi, A. Margaryan, A. Margaryan, Proc. SPIE 4974 (2003) 121.
[9] A. Margaryan, J.H. Choi, A. Margaryan, F.G. Shi, Appl. Phys. B, 78 (2004) 409.
[10] S.V.J. Lkshmn, Y.C. Ratnkaran, Phys. Chem. Glasses 29 (1988) 26.
[11] B. Viana, M. Palazzi, O. LeFol, J. Non-Cryst. Solids 215 (1997) 96.
[12] S. Jiang, T. Luo, B.C. Hwang, F. Smekatala, K. Seneschal, J. Lucas, N. Peyghambarian, J. Non-Cryst. Solids 263–264 (2000) 364.
[13] M. Weber, J.E. Lynch, D.H. Blachburn, D.J. Cronin, IEEE J. Quantum Electron. (1983) 1600.
[14] V. Petrove, U. Griebner, D. Hert, W. Seeber, Opt. Lett. 22 (1997) 365.
[15] C. Hönninger, R. Paschotta, M. Graf, M. Graf, F. Morier-Genoud, G. Zhang, M. Moser, S. Biswal, J. Nees, A. Braun, G.A. Mourou, I. Johannsen, A. Giesen, W. Seeber, U. Keller, Appl. Phys. B 69 (1999) 3.
[16] I. Yasui, H. Hagihara, H. Inoue, J. Non-Cryst. Solids 140 (1992) 130.
[17] N.L. Boling, A.J. Glass, A. Owyoung, IEEE J. Quantum Electron. (1978) 601.
[18] X. Zou, H. Toratani, Phys. Rev. B 52 (1995) 15889.
[19] S.A. Payne, L.L. Chase, L.K. Smith, et al., IEEE J. Quantum Electron. 28 (1992) 2619.
[20] H. Takebe, T. Murata, K. Morinaga, J. Am. Ceram. Soc. 79 (1996) 681.
[21] L. Zhang, H. Hu, J. Non-Cryst Solids 292 (2001) 108.
[22] L.D. Deloach, S.A. Payne, L. Smith, W.L. Kway, W.F. Krupke, J. Opt. Soc. Am. B11 (1994) 269.
[23] J. Chun, Z. Junzhou, D. Peizhen, H. Cuosong, M. Hanfen, G. Fuxi, Sci. China 42 (1999) 616.
[24] E. Fargin, A. Berthereau, T. Cardinal, G.L. Flem, L. Ducasse, L. Canioni, P. Segonds, L. Sarger, A. Ducasse, J. Non-Cryst Solids 203 (1996) 96.
[25] F. Gan, J. Non-Cryst Solids 184 (1995) 9.
[26] J.H. Choi, F.G. Shi, A. Margaryan, A. Margaryan, J. Mater. Res. 20 (1) (2005) 264–270.
[27] W. Vogel, Glass Chemistry, Springer-Verlag, 1992.
[28] W.L. Smith, The Handbook of Laser Science and Technology, Chemical Rubber Co., Boca Raton, 1989.
[29] H. Yin, P. Deng, J. Zhang, F. Gan, J. Non-Cryst. Solids 210 (1997) 243.